

Water-soluble energy harvester as a promising power solution for temporary electronic implants

Cite as: APL Mater. 8, 120701 (2020); doi: 10.1063/5.0031151
Submitted: 28 September 2020 • Accepted: 8 November 2020 •
Published Online: 1 December 2020



Qian Zhang,¹ Qijie Liang,^{1,a)}  and John A. Rogers^{2,3,a)}

AFFILIATIONS

¹Department of Physics, National University of Singapore, Singapore 117551, Singapore

²Center for Bio-Integrated Electronics, Northwestern University, Evanston, Illinois 60208, USA

³Department of Biomedical Engineering, Northwestern University, Evanston, Illinois 60208, USA

Note: This paper is part of the Special Topic on Advanced Materials and Devices for Medical Applications.

a) Authors to whom correspondence should be addressed: phylian@nus.edu.sg and jrogers@northwestern.edu

ABSTRACT

Implantable biomedical devices are rapidly advancing for applications in *in vivo* monitoring and intervention for human health. A frontier for this area is in electronic implants that function in the body for some period of time matched to an intrinsic body process and then disappear naturally, thereby avoiding the need for surgical extraction. Continuous and stable power supply to these systems is of utmost importance for their practical implementation and function. Energy harvesters that are water soluble to biocompatible end products have great potential in this context. This article presents a comprehensive review of recent progress with a focus on materials selection, device integration, and function extension. We also discuss the challenges and possible future research opportunities associated with these technologies, with a focus on implantable biomedical devices.

© 2020 Author(s). All article content, except where otherwise noted, is licensed under a Creative Commons Attribution (CC BY) license (<http://creativecommons.org/licenses/by/4.0/>). <https://doi.org/10.1063/5.0031151>

INTRODUCTION

In the past few decades, implantable biomedical devices have experienced increasing demand for human health monitoring and therapy,^{1–5} particularly in industrialized countries. An implantable biomedical device is defined as an instrument partly or completely implemented into the human body where it remains after a procedure. Many implantable biomedical devices rely fundamentally on advances in the scientific and engineering technology, and the most prominent examples are pacemakers,⁶ blood pressure sensors,⁷ and cochlear implants.⁸ The expected increasing consumers due to the coming super-aged society will further expedite the development and improvement of implantable biomedical devices.

Sources of electric power represent essential modules for implantable electronics during their normal operation. Design considerations often constrain the sizes of these systems, and their

proper function over relevant periods of time can create significant challenges in the development of appropriate power supplies. Batteries, including single-use and rechargeable types, are usually employed for such purposes. However, the high costs, large sizes, excessive weights, and/or potential risks associated with single-use batteries and their replacements and the relative lack of efficient charging schemes represent continuing challenges. With a continued shrinkage in the size and power consumption of implants, harvesting energy *in vivo* becomes an increasingly attractive potential alternative to batteries. For instance, the exploitable power from heart beating, blood flow, and lung motion may, in principle, reach levels in the range of 0.3 W–1.4 W.⁹ Transforming a small portion of these biomechanical energies into electricity could support the operation of typical sensing nodes (μ W level) and wireless communication (mW level) units in implants. In addition to kinetic energy, biochemical energy and thermal energy available in the human body represent additional

options. For example, electricity can be obtained with enzyme-modified electrodes by the oxidation of glucose and the reduction of oxygen.¹⁰

Several types of implantable energy harvesters have been reported,¹⁰ demonstrating their potential in powering implants by scavenging biomechanical energy from the human body. The fate of the energy supply module after exceeding its service period is an extremely important yet unsettled issue. This type of consideration can be addressed using the concept of transient electronics,^{11–17} where the devices and materials are designed to simply vanish over a prescribed time in a controlled manner. Water-soluble energy harvesters that combine capabilities in highly efficient energy transformation, programmed dissolvability, and biocompatibility have great potential. Although several comprehensive review articles on implantable energy harvesters are available,¹⁸ no focused review exists on water-soluble energy harvesters. To this end, this article provides an overview of the recent advances in such technologies, with a focus on materials preparation, engineering, assembly, and device integration. The extended function of these energy harvesters for health monitoring is also introduced. Moreover, the critical challenges faced by this promising technology and perspectives are highlighted throughout and in the concluding section.

SOLUBLE METALS AS FUNCTIONAL MATERIALS FOR HARVESTING RADIO FREQUENCY (RF) ENERGY

Radio waves are promising energy sources for power in many modern biomedical implants as a means to support their operation or to extend their service lifetime, with reduced possibility of infection and chemical instabilities associated with batteries. Radio frequency (RF) powered devices usually serve as part of telemetry systems for remotely measuring and transmitting data back to a central processing unit.¹⁹ Ultra-low power electronic devices in implantable biomedical systems can use harvested RF energy, typically in the high frequency (HF) range, as an energy supply to eliminate the use of batteries and to keep the sensor network free of maintenance. Wireless telemetry in biomedical implants was originally developed in the context of first-generation pacemakers. A typical system is composed of an inner-body receiving coil and an extracorporeal power transmission system. When the external coil receives RF power at the appropriate frequency, the coil produces magnetic fields within appropriate distance. On the condition that the inner inductor coil is placed with an orientation perpendicular to the external coil and the distance is suitable, some uniform electrical voltage will be generated by the magnetic flux-induced current flow through the inner coil. Although the introduction of wireless telemetry can eliminate the use of batteries, its aftertreatment after exceeding designed lifetime is an important issue to be concerned.

To solve this problem, transient RF energy harvesters have been developed by using soluble metals.²⁰ For example, Koo *et al.*²¹ reported a bioresorbable and implantable electronic system with this capability. Figures 1(a) and 1(b) display a schematic diagram and photograph of a fabricated device. The harvester is composed of a substrate of poly (lactic-co-glycolic acid) (PLGA), a RF diode based on a doped silicon nanomembrane (320 nm), and a parallel

plate capacitor with Mg as the conducting planes. The cathodic and monophasic electrical output can be obtained by modulation of the RF power applied to the transmission antenna located near the harvester. As shown in Fig. 1(c), a continuous and pulsed RF frequency power of 11 V_{pp} with a coupling distance of 80 mm applied to the transmission antenna delivers a monophasic output of 1 V. The output of the RF energy harvester can also be modulated by adjusting the distance between the harvester and the transmitter. Figure 1(d) shows the dependence of the transmitting voltage on the distance, revealing the effective control of output voltage with working distance.

The key characteristic of these systems is that all the constituent materials can be physically bioresorbed in a controlled manner and within a prescribed time when exposed to biofluids or water. Figure 1(e) shows photographs of devices at different times after being immersed in PBS at 37 °C. All the constituent materials dissolve in 3 weeks, and all the remaining residues vanish completely after 25 days. The timeline of bioresorption commencement can be well controlled by selecting the thicknesses of passive and active materials.

In addition to Mg, W can also be used in RF energy harvesters.²² As displayed in Fig. 1(f), the screen printing method can be used to fabricate the transient harvester. Tungsten conductive paste with polyethylene oxide (PEO) as a binder was screen printed on a substrate of Na-CMC, yielding wireless power harvesting and near-field communication devices (NFCs) [Fig. 1(g)]. The LED can operate with the transmitted energy from a power output of 20 W and a distance of 1 m, demonstrating the successful energy harvesting from an external RF source. Similarly, the W RF energy harvester can dissolve completely within a few minutes when exposed to water.

Despite the capability of harvesting RF energy for powering implantable biomedical devices, there are some issues that must be addressed through continued research and development. The operating range, typically less than 1 m even for high power transmission systems, represents a key limitation. In addition, reducing the size of the receiver antenna to dimensions in the millimeter range or less leads to dramatic decreases in harvesting efficiency. From a practical standpoint, wearing an external power-transferring coil or maintaining proximity to one leads to patient burden. Besides, the choice of dissolvable metals is limited, which poses restrictions on further improvements in the performance of energy harvesters and in their integration with other electronic components. The high temperature and high vacuum during metal evaporation impose additional constraints on the device design and substrate selection.

SOLUBLE SEMICONDUCTORS AS FUNCTIONAL MATERIALS FOR HARVESTING BIOMECHANICAL ENERGY

Semiconducting materials, as the foundation of modern electronics technologies, also show great potential in constructing bioresorbable energy harvesters. For example, zinc oxide with its high electron mobility, excellent transparency in the visible region, and strong piezoelectric response has been intensively explored in light emitting devices, piezoelectric transducers,²³ photodetectors,^{24,25} and strain sensors.^{26–28} The biocompatibility and water

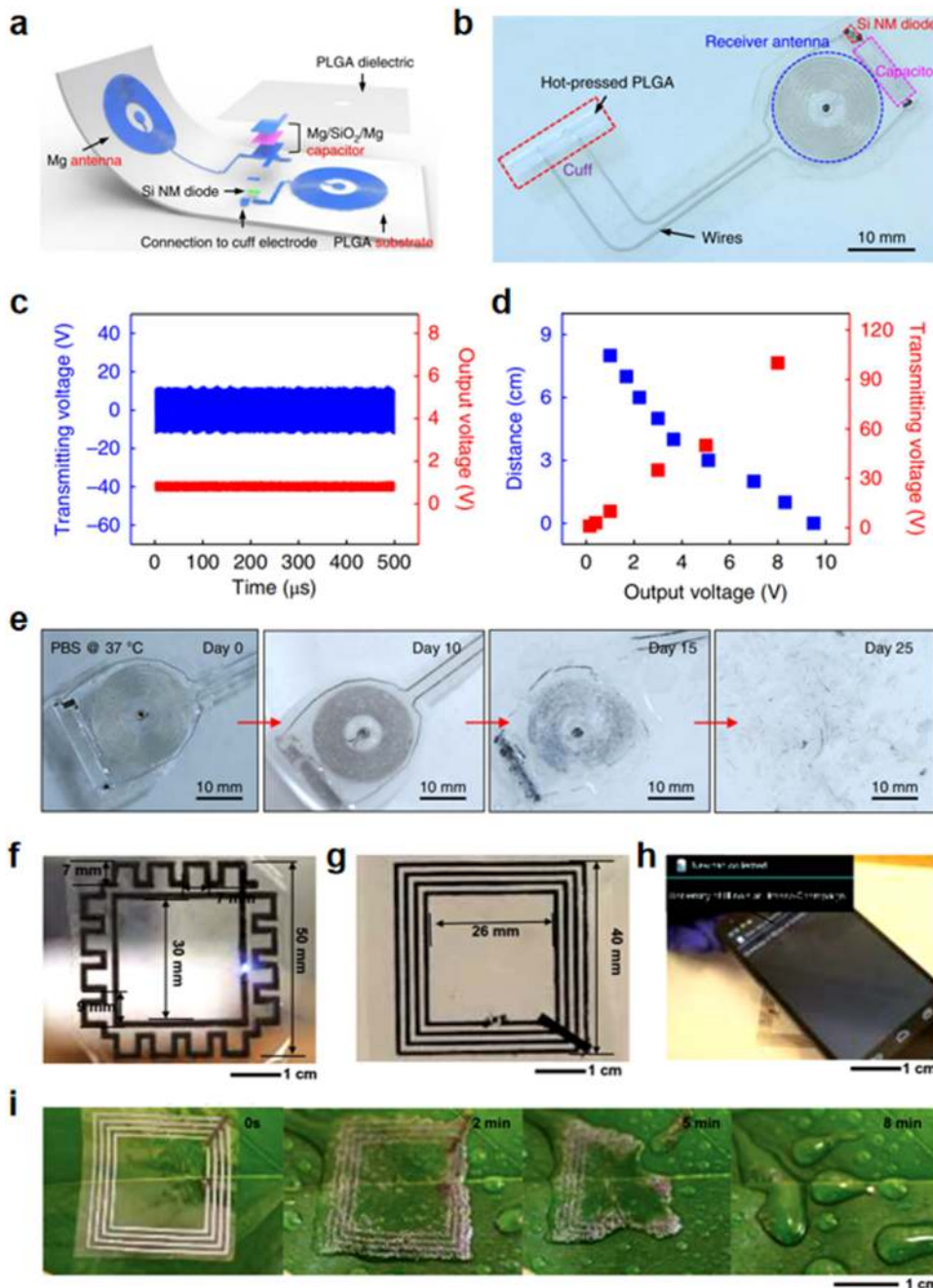


FIG. 1. Soluble energy harvester for scavenging radio frequency energy. (a) Schematic diagram of a bioresorbable wireless electrical stimulator that can harvest RF energy. The wireless receiver consists of a RF diode, a capacitor, and an inductor. PLGA serves as the substrate. (b) Photograph of the fabricated device. (c) Typical output waveform wirelessly generated by an alternating current from the transmission coil. (d) Dependence of the output voltage on the distance between the harvester and the transmitter. (e) Dissolution of the bioresorbable wireless RF energy harvester in PBS at 37 °C. Reproduced with permission from Koo *et al.*, *Nat. Med.* **24**, 1830 (2018). Copyright 2018 Nature Publishing Group. (f) Printed soluble RF power harvesting circuit with a meander loop antenna formed using a screen-printed W paste. (g) A soluble NFC circuit with an inductive coupling coil. (h) Photograph demonstrating readout of the NFC circuit with a cellphone. (i) Dissolution of the soluble NFC coil on a leaf by a spray of water. Reproduced with permission from Huang *et al.*, *Adv. Mater.* **26**, 7371 (2014). Copyright 2014 Wiley-VCH.

solubility, via hydrolysis, of ZnO have been reported by previous works, showing its potential for integrating on or in the human body.

Dagdeviren *et al.* introduced a soluble energy harvester with a ZnO film as the active material, silk fibroin as the substrate and package, magnesium as the electrodes and interconnects, and magnesium oxide as the dielectric.²⁹ A schematic diagram of the ZnO energy harvester is depicted in Fig. 2(a). Figure 2(b) presents an

image of an array of ZnO energy harvesters with a capacitor-type geometry. When subjected to a compressive force, the harvester mechanically buckles upward, generating a non-uniform bending moment. The piezoelectric effect in ZnO coupled with mechanical deformation induces a potential difference in the top and bottom Mg electrodes. This potential can drive the flow of electrons through an external circuit, corresponding to the alternating signal in Figs. 2(c) and 2(d). The voltage and current from this particular example of

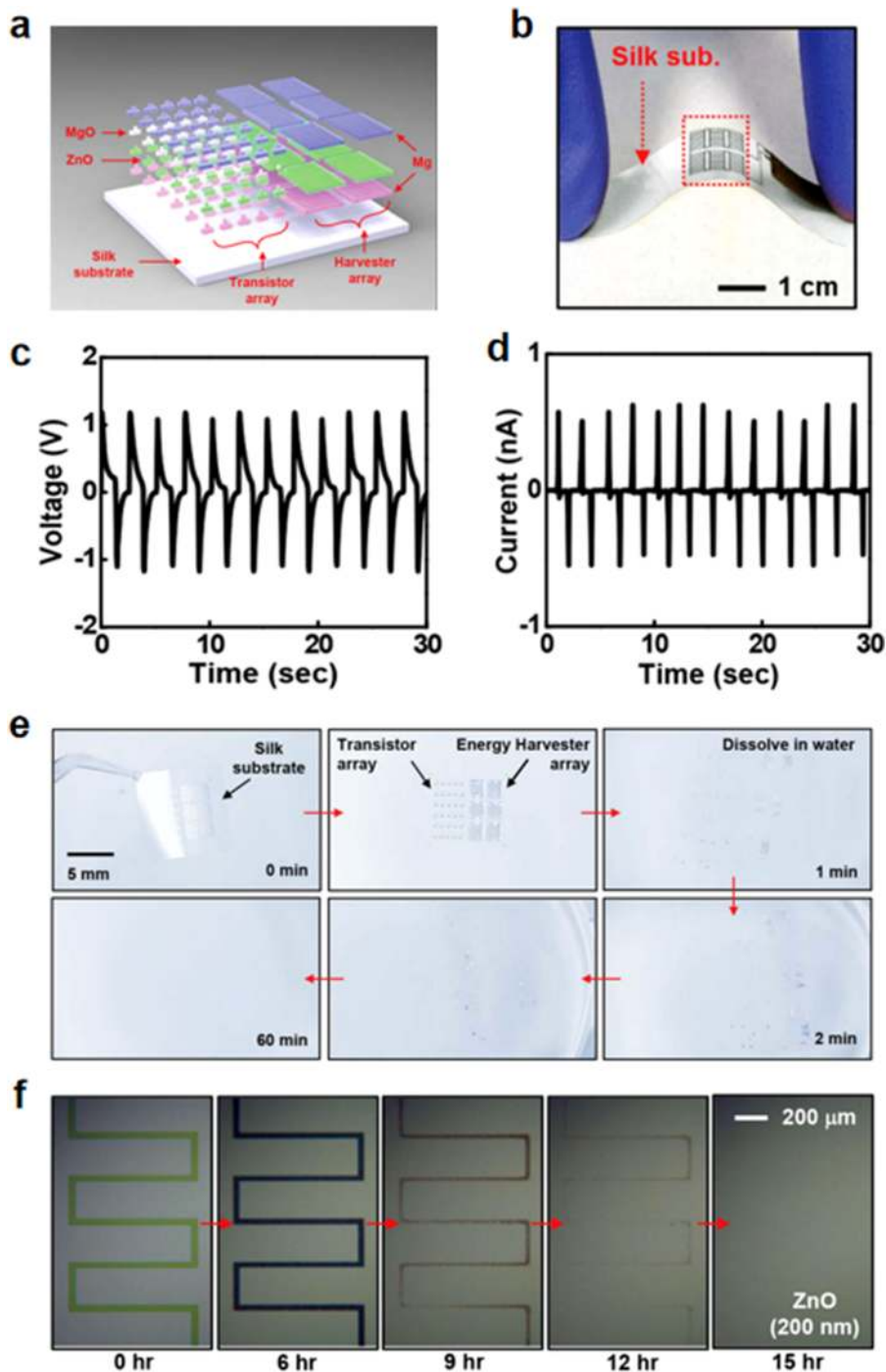


FIG. 2. Water-soluble energy harvester based on a piezoelectric material. (a) Schematic diagram of a bioresorbable ZnO mechanical energy harvester. (b) Photograph of a fabricated ZnO energy harvester on a thin film silk substrate in a bent configuration. (c) Typical output voltage and (d) current during cycles of bending. (e) Dissolution of a bioresorbable ZnO energy harvester in water at room temperature. (f) Optical microscope images at various times during dissolution of a meander trace of ZnO (200 nm) in deionized water at room temperature. Reproduced with permission from Dagdeviren *et al.*, *Small* **9**, 3398 (2013). Copyright 2013 Wiley-VCH.

a ZnO energy harvester reach 1.14 V and 0.55 nA, respectively. The calculated efficiency for mechanical to electrical energy conversion is 0.28%, which represents a promising result that might be improved through additional work, as the potential basis for a practical supply of energy.

Investigations of the solubility of a ZnO energy harvester are shown in Fig. 2(e). After being exposed to deionized water at room temperature, the silk substrate quickly disappears, resulting in physical disintegration of the whole device structure. Subsequently, all the constituent materials start to dissolve due to hydrolysis at different

rates. In particular, the hydrolysis of a meander trace of ZnO as a function of time is presented in Fig. 2(f). The product of hydrolysis of ZnO is $[\text{Zn}(\text{OH})_2]$. The reaction for this specific example runs to completion within 15 h.

There are some limitations with a semiconductor-based soluble energy harvester. The output power is usually low due to their small piezoelectric coefficient. In addition, the fabrication process is relatively complicated compared to that for energy harvesters composed of simply metals and polymers, as an additional barrier to large-scale preparation and practical application.

SOLUBLE POLYMERS AS FUNCTIONAL MATERIALS FOR HARVESTING BIOMECHANICAL ENERGY

Before the invention of triboelectric energy harvesters, polymers were usually used as substrates or encapsulation layers. Triboelectric nanogenerator based on the coupling of the triboelectric effect and electrostatic effect allows for use of polymers as active materials for mechanical energy harvesting^{30–33} and self-powered sensors.³⁴ The simple structure, high efficiency, excellent robustness, and cost-effectiveness of triboelectric nanogenerators are promising attributes for use in biomechanical energy harvesting, blue energy harvesting, human movement detection, and human health protection.³⁵ By selecting soluble constituent materials and rationally designing the reactions with surrounding solvents such as water, a triboelectric energy harvester can be constructed in water soluble and biocompatible forms, with promising potential for use as energy supplements for electronic biomedical implants.

Liang *et al.*³⁶ developed a green and recyclable triboelectric energy harvester with planar configuration, as shown in Fig. 3(a). The device structure is composed of sodium alginate (SA) and polyvinyl alcohol (PVA) as functional materials and aluminum and lithium as electrodes. Figure 3(b) presents the water-triggered dissolution process of the harvester. When exposed to water, the encapsulation layer of the soluble tape will first dissolve. Then, water reacts with the lithium electrode to generate hydrogen gas, thereby accelerating the entire dissolution process. Simultaneously, contact materials of PVA and SA films decompose through interactions with the surrounding water. Finally, the aluminum electrode is removed with LiOH produced by reactions between lithium and water. Therefore, the entire device completely decomposes through this cascade of processes.

Mechanisms of transforming biomechanical energy to electricity are depicted in Fig. 3(c). External mechanical motion triggers periodic contact and separation between two contact materials, which induces potential differences between the two corresponding electrodes. Thus, alternating currents are generated as a result of electron transfer between the two electrodes, driven by an electrical potential difference. Typical output voltages and currents are displayed in Figs. 3(d) and 3(e), which can reach 2.6 V and 18 nA when triggered by a simple press of the finger. This distinct working mechanism leads to output power densities that can be much higher than those of piezoelectric harvesters such as the ZnO device described previously.^{37,38} The dissolution of the fabricated device was also studied, as shown in the optical images at various times during decomposition of the harvester in deionized water at room

temperature [Figs. 3(f)–3(h)]. The energy harvester decomposes in less than 10 min.

The other interesting feature of this soluble energy harvester is that the products of dissolution do not need to be discharged into our environment but instead can be captured and used to reproduce the energy harvester. The influence on the environment was investigated with suspended solids and chemical oxygen demand that is widely used as an indicator to identify the characteristics of waste water by quantifying the amount of organics in water.³⁹ The maximum values of the suspended solids and chemical oxygen demand are 143 mg/l and 70 mg/l, respectively. These results indicate that this type of soluble energy harvester is eco-friendly, with potential for further improvements by size miniaturization and materials replacement. The products of dissolution can be re-deposited to reproduce the membrane as the contact materials of the harvester. The dielectric constant of the reproduced membrane was found to be comparable to that of the original membrane. The output voltage of the reproduced soluble energy harvester is also comparable to that of the original.

Zheng *et al.*⁴⁰ also developed a soluble and implantable energy harvester based on biodegradable polymers. The device incorporates a multilayer structure, in which biodegradable polymers serve as contact materials and resorbable metals act as electrodes, as schematically illustrated in Fig. 4(a). The biocompatibility of the constituent materials is investigated by culturing endotheliocytes on the prepared polymer films. As shown in Fig. 4(b), most of the cells are viable and display no obvious difference with the control group after seven days of culture. The detection of intact cytoskeletal structures suggests that most of the cells are healthy. *In vitro* biodegradation tests are performed to study the device absorption characteristics. Energy harvesters with different encapsulation materials are exposed to a PBS buffer at 37 °C. At first, the encapsulation layer of PLGA will gradually swell, following by the penetration of water into the inner structure of the harvester. Finally, the entire device disappears within 90 days.

The *in vivo* degradation and evaluation of cellular and tissue responses are of great importance in the design and development of biodegradable devices. Thus, a representative energy harvester encapsulated in a PLGA film was implanted into the subdermal region of a rat, as shown in Fig. 4(d). The surgical site healed well, and no obvious signs of infection were observed after 9 weeks of implantation, indicating the excellent biocompatibility of the energy harvester. The histological section in Fig. 4(e) displays the site of the device, located between the muscle layer and the subdermal layer with some surrounding fibrous tissues. No significant inflammatory reaction was observed.

The mechanism of transforming biomechanical energy to electricity relies on coupling between triboelectrification and electrostatic induction, similar to that described previously.^{41–43} Figure 4(f) presents the typical output voltage and current of devices with various polymers as contact materials. The maximum voltage and current can reach 40 V and 1 μA and can be modulated across a large range by simply changing the contact materials. The *in vivo* characterization on the output performance of the implanted energy harvester was also investigated. As shown in Fig. 4(g), the output voltage of the PLGA-encapsulated energy harvester decreased from 4 V to 1 V after 2 weeks of implantation. This degradation arises from restrictions in motion imposed by a fibrous capsule that forms

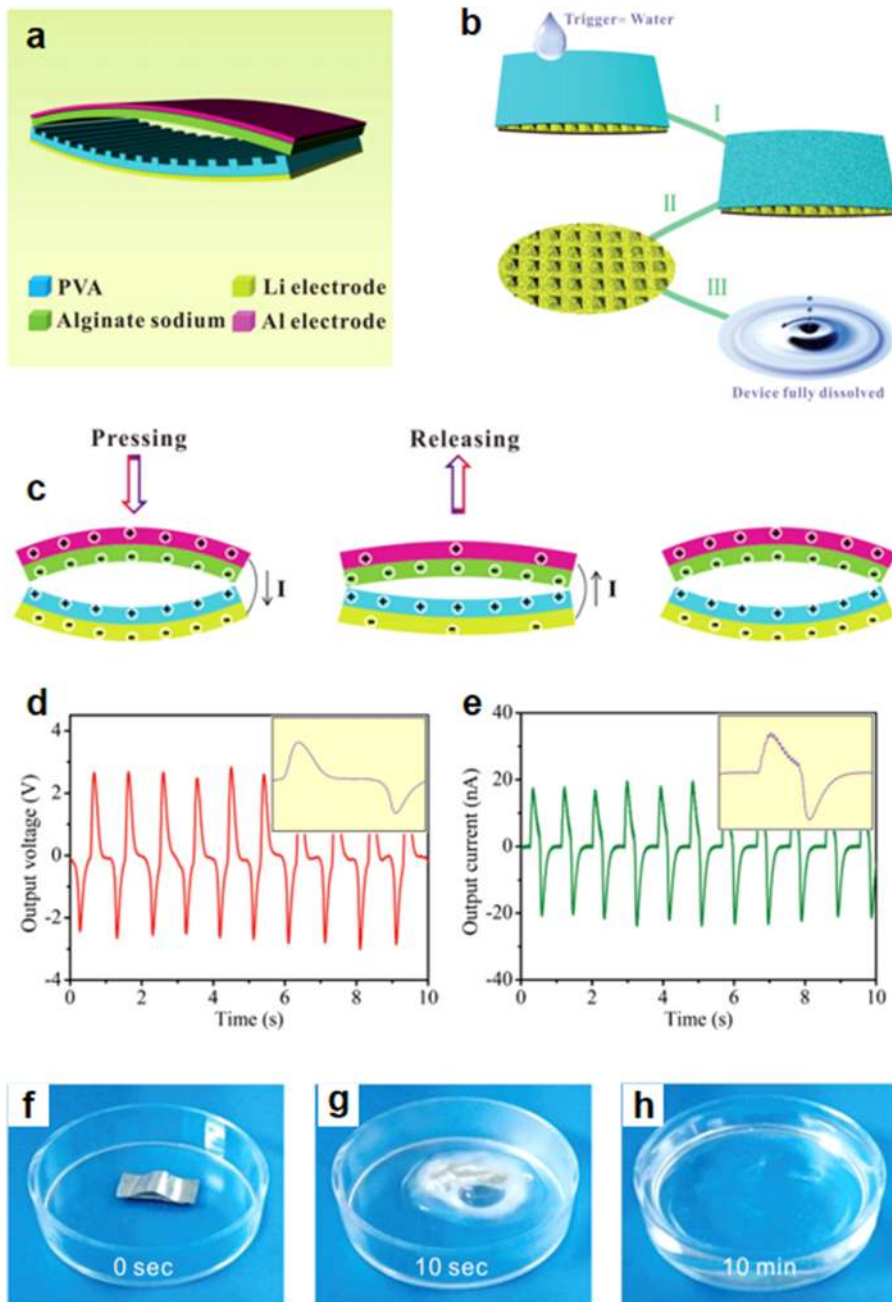


FIG. 3. Water-soluble triboelectric energy harvester based on dissolvable polymers. (a) Schematic diagram of the soluble triboelectric energy harvester. (b) Dissolution mechanism of the harvester. (c) Energy harvesting mechanism. (d) Typical output voltage and (e) current from the harvester. (f)–(h) Optical images at various times during dissolution of the harvester in deionized water at room temperature. Reproduced with permission from Liang *et al.*, *Adv. Mater.* **29**, 1604961 (2017). Copyright 2017 Wiley-VCH.

around the devices and from the decomposition of encapsulation materials.

Other papers report additional attempts to develop biodegradable polymer-based energy harvesters.^{44,45} For example, Chi *et al.*⁴⁶ fabricated a rice paper-based energy harvester. An image of a piece of rice paper and a schematic diagram of the device are shown in Figs. 5(a) and 5(b). The maximum open-circuit voltage and

short-circuit current reach 244 V and 6 μ A, with a power density of 37.6 μ W/cm². Bao *et al.*⁴⁷ developed a lignin biopolymer-based energy harvester. The contact materials are the lignin–starch nanocomposite [Fig. 5(c)] and PVA film, as schematically illustrated in Fig. 5(d). A power density of 173.5 nW/cm² was achieved with this device. Lu *et al.*⁴⁸ demonstrated a pullulan-based recyclable energy harvester. Figure 5(e) displays a photograph of a pullulan-based

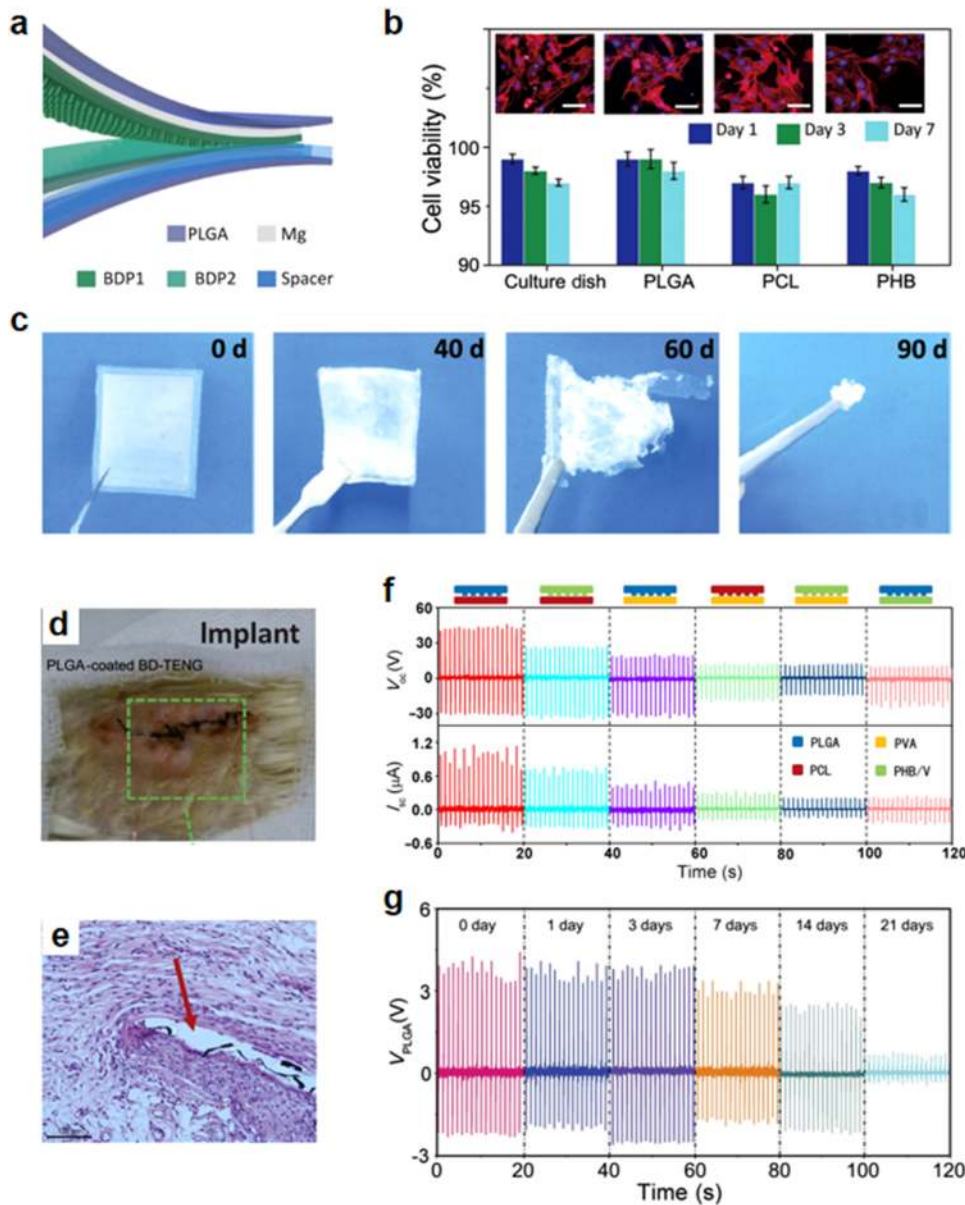


FIG. 4. (a) Schematic diagram of a biodegradable energy harvester. (b) Biocompatibility test with endothelial cells of biodegradable polymers for seven days. (The inset shows fluorescence images of stained cells. Scale bar: 100 μm .) (c) Photographs of a fabricated device at various times in PBS at 37 °C. (d) Images of an implanted device located in the subdermal dorsal region of a rat. (e) Histological section of tissue at the implant site after 9 weeks, revealing a partially resorbed region of the energy harvester. (f) Output performance of the energy harvesters with different biodegradable contact materials. (g) Electrical output of a device that was encapsulated in PLGA. Reproduced with permission from Zheng *et al.*, *Sci. Adv.* **2**, e1501478 (2016). Copyright 2016 American Association for the Advancement of Science.

film. The maximum output voltage and power density are 79 V and 41.7 mW/m^2 , as achieved with the device structure shown in Fig. 5(f). Kim *et al.*⁴⁹ developed a silk fibroin-based energy harvester by incorporating ferroelectric nanoparticles into its matrix. Figure 5(g) presents schematic diagrams of the fabrication process and the structure of the device. The maximum output voltage and current densities are 2.2 V and 0.12 $\mu\text{A}/\text{cm}^2$, respectively. Another biodegradable polymer, a gelatin film, was also applied in an energy harvester.⁵⁰ As illustrated in Fig. 5(h), the gelatin film and a film of poly lactic acid (PLA) served as contact materials. The reported output voltages are as high as 500 V, and the power densities are 5 W/m^2 for devices with dimensions of 4 \times 4 cm^2 .

Biodegradable polymers have been extensively studied in energy harvesters that use the triboelectric effect. However, the dimensions of this kind of device are typically in the cm range, and a further size reduction is required to integrate with other functional components in biomedical implants.

SOLUBLE ENERGY HARVESTER WITH SELF-POWERED SENSING AND THERAPY FUNCTION

In addition to harvesting biomechanical energy for energy supply to implantable devices/systems, the harvesters can also serve as

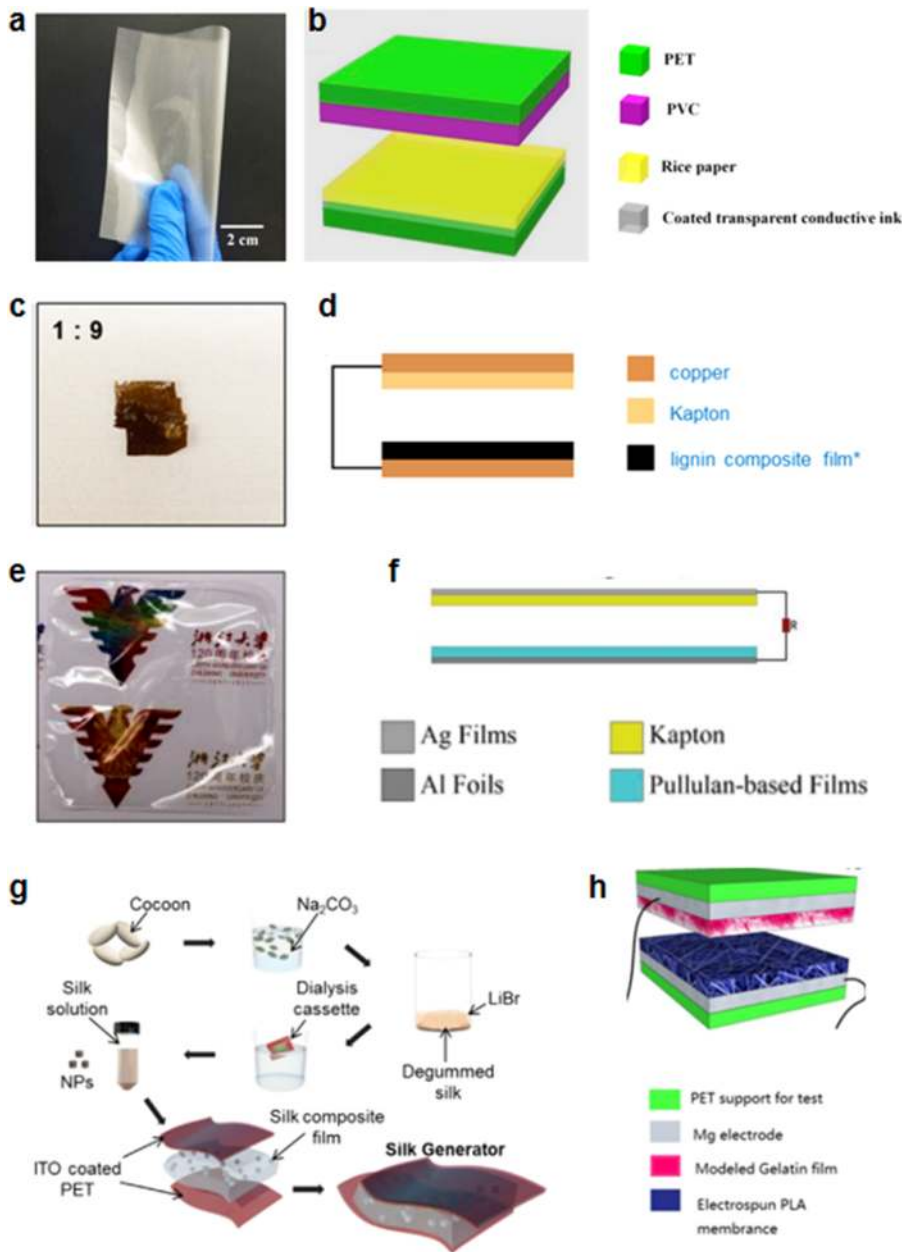


FIG. 5. Energy harvesters with biodegradable polymers as functional materials. (a) Photograph of a piece of rice paper. (b) Schematic diagram of a rice paper-based energy harvester. Reproduced with permission from Chi *et al.*, *Microelectron. Eng.* **216**, 111059 (2019). Copyright 2016 Elsevier. (c) Photographs of lignin-starch films. Scale bar: 3.5 cm. (d) Schematic diagram of a lignin biopolymer-based energy harvester. Reproduced with permission from Bao *et al.*, *APL Mater.* **5**, 074109 (2017). Copyright 2017 AIP Publishing LLC. (e) Photograph of a pullulan-based film. (f) Schematic diagram of a pullulan-based energy harvester. Reproduced with permission from Lu *et al.*, *Adv. Mater. Technol.* **5**, 1900905 (2020). Copyright 2020 Wiley-VCH. (g) Schematic diagrams of the fabrication process of the silk fibroin-based energy harvester. Reproduced with permission from Kim *et al.*, *Nano Energy* **14**, 87 (2015). Copyright 2015 Elsevier. (h) Schematic diagram of the gelatin and PLA-based energy harvester. Reproduced with permission from Pan *et al.*, *Nano Energy* **45**, 193 (2018). Copyright 2018 Elsevier.

the basis of self-powered health monitors or of devices that provide therapy to the human body. Figure 6(a) shows an image of a soluble energy harvester attached to the lungs to transform its biomechanical energy to electricity.³⁶ When any human organ periodically contracts and expands, a corresponding alternating current can be generated, as displayed in Fig. 6(b). Therefore, analyzing the voltage or current signal of an energy harvester can serve as a metric for the health status of those human organs.

Electricity generated from soluble energy harvesters can also be used for enhanced neuroregeneration and functional recovery.

Koo *et al.*²¹ reported a wireless bioresorbable electronic system for sustained non-pharmacological neuroregenerative therapy. As previously described, electrical signals can be delivered by passing radio frequency power through a transmission antenna. Figure 6(c) shows a photograph of a bioresorbable wireless stimulator for skeletal muscle and a surgical image of the implantation. Electromyograms (EMGs)^{51,52} were recorded to investigate the regeneration of sciatic nerves injured by transection. A series of EMGs obtained from the tibialis anterior muscle at various stages after surgery with and without stimulation appear in Fig. 6(d).

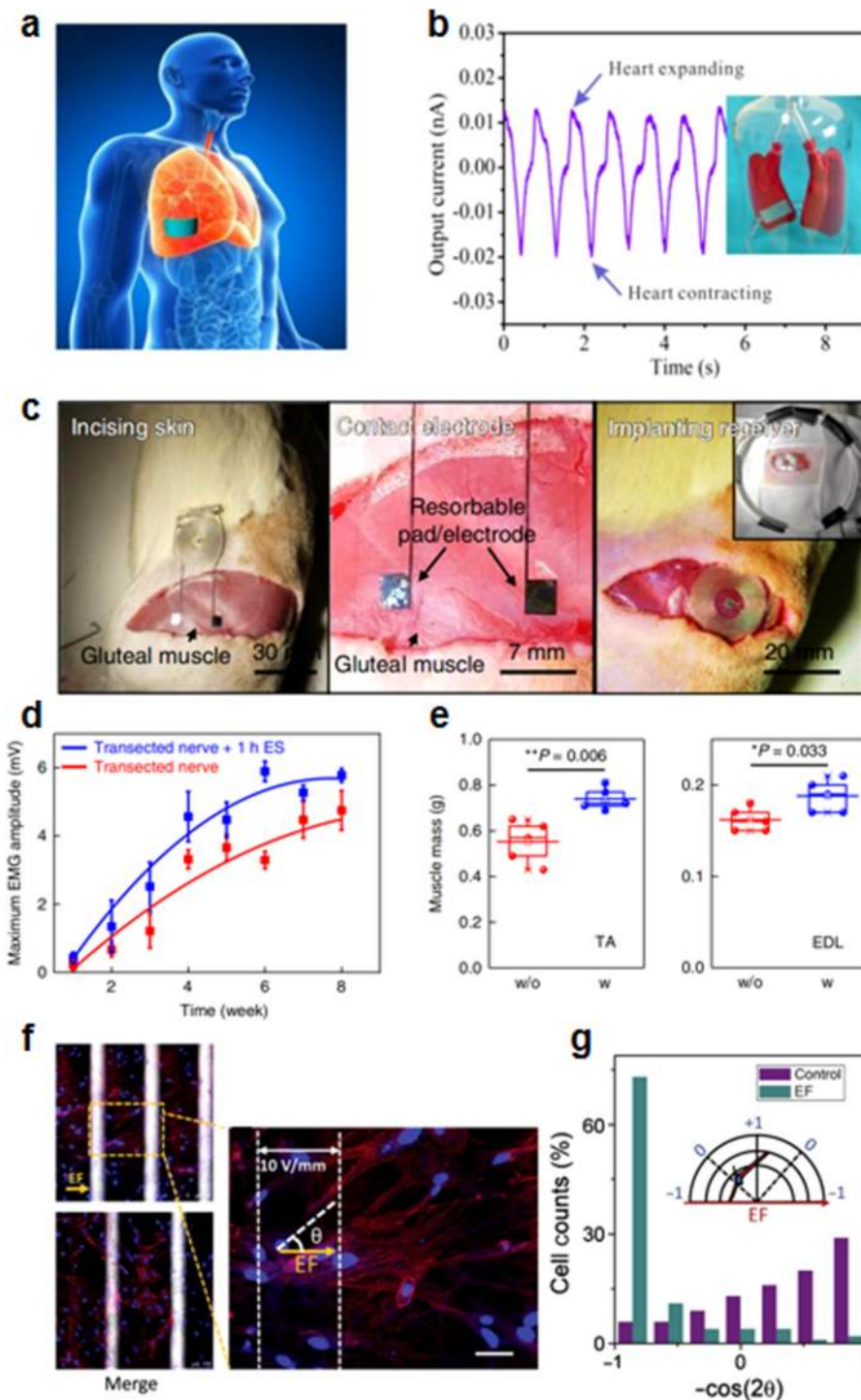


FIG. 6. Soluble energy harvesters for health monitoring and therapy. (a) Schematic illustration of a soluble energy harvester attached on the human organ. (b) Output current from a soluble device attached on a plastic model for simulating cardiac activity or human respiration. Reproduced with permission from Liang *et al.*, *Adv. Mater.* **29**, 1604961 (2017). Copyright 2017 Wiley-VCH. (c) Photograph of a bioresorbable wireless stimulator for skeletal muscles and surgical image of implantation. (d) Maximum EMG amplitudes obtained from the tibialis anterior muscle after transection/direct repair of the sciatic nerve. (e) Muscle mass measurements obtained at 8 weeks after implantation following electrical stimulation in the tibialis anterior and EDL muscles. Reproduced with permission from Koo *et al.*, *Nat. Med.* **24**, 1830 (2018). Copyright 2018 Nature Publishing Group. (f) Orientation and distribution of nerve cells cultured on the electrodes of a triboelectric energy harvester. Scale bar: $50 \mu\text{m}$. (g) Cell alignment analysis where the cell angle is represented by $-\cos(2\theta)$. Reproduced with permission from Zheng *et al.*, *Sci. Adv.* **2**, e1501478 (2016). Copyright 2016 American Association for the Advancement of Science.

Greater muscle activation in the tibialis anterior is observed in the presence of stimulation comparing with its absence for all stages of recovery. Figure 6(e) presents muscle mass measurements obtained at 8 weeks after implantation following electrical stimulation in the

tibialis anterior and extensor digitorum longus (EDL) muscles. Similar improvements by electrical stimulation are also observed after 8 weeks following the injury. These results illustrate the capability of implantable wireless bioresorbable electronic systems to improve

nerve regeneration and function recovery compared to negative controls.

The utilization of electric stimulation in tissue engineering is also reported with a soluble triboelectric energy harvester.⁴⁰ Zheng *et al.* applied electrical signals from triboelectric energy harvesters as stimulation to improve neuron cell orientation. Figure 6(f) displays the orientation and distribution of nerve cells cultured on the electrodes of a triboelectric energy harvester. The well-oriented neurons align parallel to the electric field. In contrast, the cell arrangement and cyto-skeleton structures have no obvious orientation in the control group. The angle between a line drawn through the long axis of the cell and 0° is recorded, and $-\cos 2\theta$ is employed as a convenient description of cell alignment. As shown in Fig. 6(g), when stimulated with an electric field, an obvious tendency of alignment is presented in comparison to the randomly distributed cell angles without electrical stimulation.

CONCLUSIONS AND PERSPECTIVES

Here, we reviewed recent progress in the development of soluble energy harvesters with potential in powering implantable biomedical devices/systems. From the materials' point of view, bioresorbable metals, semiconductors, and polymers have been successfully deployed as functional materials to construct biocompatible energy harvesters that effectively scavenge RF or biomechanical energy. In addition to energy supply for implants, soluble energy harvesters can also serve as health monitors or as therapeutic devices for applications in nerve regeneration, tissue repair, and others. Due to increased output power and extended multifunctionality, successful demonstration of soluble energy harvesters and their integration with other electronic devices/systems suggests practical potential for use in various areas of human healthcare, with possibilities for commercialization. Nevertheless, several critical issues remain to be addressed through continued research and development, as follows:

- (1) Efficiency improvement: Although the output of certain classes of bioresorbable energy harvesters can reach the mW level, others are in the range of nW to μ W. Strategies for utilizing new bioresorbable materials, for using physical and chemical engineering principles to improve their intrinsic properties, and schemes for a rational device configuration design should be explored. In addition to the mechanical source of energy, multimodal devices that also exploit thermal and chemical sources of energy that are abundant in the human body offer great potential.
- (2) Power management: To utilize the outputs from the classes of soluble energy harvesters reviewed here, regulation of the voltage/current amplitudes and polarity is typically required. For example, the alternating current from triboelectric energy harvesters must be transformed to direct current with appropriate converters for practical application. Therefore, soluble converter and other electronics are desirable. Certain semiconducting two-dimensional materials that possess bioresorbability and the capability for integration into various devices are promising candidates.^{53–56} For example, a MoS₂-enabled flexible rectenna⁵⁷ for Wi-Fi-band wireless energy

harvesting has been reported, and the biocompatibility and bioresorbability of MoS₂ were also demonstrated by previous work.⁵⁸

- (3) Long-term service behavior: Many experiments to characterize soluble energy harvesters are performed *in vitro* or in simulated environments. The influence of the complex biochemical and biomechanical environments encountered in living systems, including chemical, thermal, and biomechanical effects, on the performance must be carefully investigated. In addition, the stability of operation and power output must be explored in the context of designed lifetime requirements.
- (4) Long-term influence on biological systems: Most biocompatibility tests on previously reported soluble energy harvesters are based on *in vitro* experiments and/or small animal models. The influence of soluble devices on relevant biological environments, such as vital organs, muscles, and contacting tissues, should be further examined. Besides, with the development of soluble energy harvesters, new materials or devices/systems are required to ensure full system operational characteristics that address practical needs. Additional research efforts are needed to quantitatively understand the impacts of the materials and devices on biological systems and to minimize the potential influences of materials engineering and system optimization aspects.

ACKNOWLEDGMENTS

This mini-review was not supported by funding.

DATA AVAILABILITY

The data that support the findings of this study are available from the corresponding author upon reasonable request.

REFERENCES

- ¹S. I. Park, D. S. Brenner, G. Shin, C. D. Morgan, B. A. Copits, H. U. Chung, M. Y. Pullen, K. N. Noh, S. Davidson, S. J. Oh, J. Yoon, K.-I. Jang, V. K. Samineni, M. Norman, J. G. Grajales-Reyes, S. K. Vogt, S. S. Sundaram, K. M. Wilson, J. S. Ha, R. Xu, T. Pan, T.-i. Kim, Y. Huang, M. C. Montana, J. P. Golden, M. R. Bruchas, R. W. Gereau, and J. A. Rogers, *Nat. Biotechnol.* **33**, 1280 (2015).
- ²S. M. Won, E. Song, J. T. Reeder, and J. A. Rogers, *Cell* **181**, 115 (2020).
- ³S.-W. Hwang, J.-K. Song, X. Huang, H. Cheng, S.-K. Kang, B. H. Kim, J.-H. Kim, S. Yu, Y. Huang, and J. A. Rogers, *Adv. Mater.* **26**, 3905 (2014).
- ⁴D.-H. Kim, Y.-S. Kim, J. Amsden, B. Panilaitis, D. L. Kaplan, F. G. Omenetto, M. R. Zakin, and J. A. Rogers, *Appl. Phys. Lett.* **95**, 133701 (2009).
- ⁵S.-K. Kang, R. K. J. Murphy, S.-W. Hwang, S. M. Lee, D. V. Harburg, N. A. Krueger, J. Shin, P. Gamble, H. Cheng, S. Yu, Z. Liu, J. G. McCall, M. Stephen, H. Ying, J. Kim, G. Park, R. C. Webb, C. H. Lee, S. Chung, D. S. Wie, A. D. Gujar, B. Vemulapalli, A. H. Kim, K.-M. Lee, J. Cheng, Y. Huang, S. H. Lee, P. V. Braun, W. Z. Ray, and J. A. Rogers, *Nature* **530**, 71 (2016).
- ⁶P. Gutruf, R. T. Yin, K. B. Lee, J. Ausra, J. A. Brennan, Y. Qiao, Z. Xie, R. Peralta, O. Talarico, A. Murillo, S. W. Chen, J. P. Leshock, C. R. Haney, E. A. Waters, C. Zhang, H. Luan, Y. Huang, G. Trachiotis, I. R. Efimov, and J. A. Rogers, *Nat. Commun.* **10**, 5742 (2019).
- ⁷P. Starr, K. Bartels, C. M. Agrawal, and S. Bailey, *Sens. Actuators, A* **248**, 38 (2016).

- ⁸B. İlik, A. Koyuncuoğlu, Ö. Şardan-Sukas, and H. Kùlah, *Sens. Actuators, A* **280**, 38 (2018).
- ⁹J. Li and X. Wang, *APL Mater.* **5**, 073801 (2017).
- ¹⁰B. Shi, Z. Li, and Y. Fan, *Adv. Mater.* **30**, 1801511 (2018).
- ¹¹D.-H. Kim, J. Viveni, J. J. Amsden, J. Xiao, L. Vigeland, Y.-S. Kim, J. A. Blanco, B. Panilaitis, E. S. Frechette, D. Contreras, D. L. Kaplan, F. G. Omenetto, Y. Huang, K.-C. Hwang, M. R. Zakin, B. Litt, and J. A. Rogers, *Nat. Mater.* **9**, 511 (2010).
- ¹²D.-H. Kim, R. Ghaffari, N. Lu, and J. A. Rogers, *Annu. Rev. Biomed. Eng.* **14**, 113 (2012).
- ¹³C. Dagdeviren, B. D. Yang, Y. Su, P. L. Tran, P. Joe, E. Anderson, J. Xia, V. Doraiswamy, B. Dehdashti, X. Feng, B. Lu, R. Poston, Z. Khalpey, R. Ghaffari, Y. Huang, M. J. Slepian, and J. A. Rogers, *Proc. Natl. Acad. Sci. U. S. A.* **111**, 1927 (2014).
- ¹⁴S.-W. Hwang, C. H. Lee, H. Cheng, J.-W. Jeong, S.-K. Kang, J.-H. Kim, J. Shin, J. Yang, Z. Liu, G. A. Ameer, Y. Huang, and J. A. Rogers, *Nano Lett.* **15**, 2801 (2015).
- ¹⁵Z. Xie, R. Avila, Y. Huang, and J. A. Rogers, *Adv. Mater.* **32**, 1902767 (2020).
- ¹⁶S. M. Won, J. Koo, K. E. Crawford, A. D. Mickle, Y. Xue, S. Min, L. A. McIlvried, Y. Yan, S. B. Kim, S. M. Lee, B. H. Kim, H. Jang, M. R. MacEwan, Y. Huang, R. W. Gereau, and J. A. Rogers, *Adv. Funct. Mater.* **28**, 1801819 (2018).
- ¹⁷S.-W. Hwang, H. Tao, D.-H. Kim, H. Cheng, J.-K. Song, E. Rill, M. A. Brenckle, B. Panilaitis, S. M. Won, Y.-S. Kim, Y. M. Song, K. J. Yu, A. Ameen, R. Li, Y. Su, M. Yang, D. L. Kaplan, M. R. Zakin, M. J. Slepian, Y. Huang, F. G. Omenetto, and J. A. Rogers, *Science* **337**, 1640 (2012).
- ¹⁸M. A. Hannan, S. Mutashar, S. A. Samad, and A. Hussain, *BioMed. Eng. OnLine* **13**, 79 (2014).
- ¹⁹S.-W. Hwang, X. Huang, J.-H. Seo, J.-K. Song, S. Kim, S. Hage-Ali, H.-J. Chung, H. Tao, F. G. Omenetto, Z. Ma, and J. A. Rogers, *Adv. Mater.* **25**, 3526 (2013).
- ²⁰L. Yin, H. Cheng, S. Mao, R. Haasch, Y. Liu, X. Xie, S.-W. Hwang, H. Jain, S.-K. Kang, Y. Su, R. Li, Y. Huang, and J. A. Rogers, *Adv. Funct. Mater.* **24**, 645 (2014).
- ²¹J. Koo, M. R. MacEwan, S.-K. Kang, S. M. Won, M. Stephen, P. Gamble, Z. Xie, Y. Yan, Y.-Y. Chen, J. Shin, N. Birenbaum, S. Chung, S. B. Kim, J. Khalifeh, D. V. Harburg, K. Bean, M. Paskett, J. Kim, Z. S. Zohny, S. M. Lee, R. Zhang, K. Luo, B. Ji, A. Banks, H. M. Lee, Y. Huang, W. Z. Ray, and J. A. Rogers, *Nat. Med.* **24**, 1830 (2018).
- ²²X. Huang, Y. Liu, S.-W. Hwang, S.-K. Kang, D. Patnaik, J. F. Cortes, and J. A. Rogers, *Adv. Mater.* **26**, 7371 (2014).
- ²³S. Lu, Q. Liao, J. Qi, S. Liu, Y. Liu, Q. Liang, G. Zhang, and Y. Zhang, *Nano Res.* **9**, 372 (2016).
- ²⁴S. Lu, J. Qi, S. Liu, Z. Zhang, Z. Wang, P. Lin, Q. Liao, Q. Liang, and Y. Zhang, *ACS Appl. Mater. Interface* **6**, 014116 (2014).
- ²⁵S. Lu, J. Qi, Y. Gu, S. Liu, Q. Xu, Z. Wang, Q. Liang, and Y. Zhang, *Nanoscale* **7**, 4461 (2015).
- ²⁶X. Zheng, X. Yan, Y. Sun, Z. Bai, G. Zhang, Y. Shen, Q. Liang, and Y. Zhang, *ACS Appl. Mater. Inter.* **7**, 2480 (2015).
- ²⁷S. Cao, X. Yan, Z. Kang, Q. Liang, X. Liao, and Y. Zhang, *Nano Energy* **24**, 25 (2016).
- ²⁸X. Liao, Q. Liao, Z. Zhang, X. Yan, Q. Liang, Q. Wang, M. Li, and Y. Zhang, *Adv. Funct. Mater.* **26**, 3074 (2016).
- ²⁹C. Dagdeviren, S.-W. Hwang, Y. Su, S. Kim, H. Cheng, O. Gur, R. Haney, F. G. Omenetto, Y. Huang, and J. A. Rogers, *Small* **9**, 3398 (2013).
- ³⁰Q. Liang, X. Yan, Y. Gu, K. Zhang, M. Liang, S. Lu, X. Zheng, and Y. Zhang, *Sci. Rep.* **5**, 9080 (2015).
- ³¹M. Ma, Q. Liao, G. Zhang, Z. Zhang, Q. Liang, and Y. Zhang, *Adv. Funct. Mater.* **25**, 6489 (2015).
- ³²Q. Liang, X. Yan, X. Liao, S. Cao, X. Zheng, H. Si, S. Lu, and Y. Zhang, *Nano Energy* **16**, 329 (2015).
- ³³Q. Zhang, Q. Liang, Q. Liao, M. Ma, F. Gao, X. Zhao, Y. Song, L. Song, X. Xun, and Y. Zhang, *Adv. Funct. Mater.* **28**, 1803117 (2018).
- ³⁴Q. Liang, Z. Zhanga, X. Yan, Y. Gu, Y. Zhao, G. Zhang, S. Lu, Q. Liao, and Y. Zhang, *Nano Energy* **14**, 209 (2015).
- ³⁵Q. Zhang, Q. Liang, Z. Zhang, Z. Kang, Q. Liao, Y. Ding, M. Ma, F. Gao, X. Zhao, and Y. Zhang, *Adv. Funct. Mater.* **28**, 1703801 (2018).
- ³⁶Q. Liang, Q. Zhang, X. Yan, X. Liao, L. Han, F. Yi, M. Ma, and Y. Zhang, *Adv. Mater.* **29**, 1604961 (2017).
- ³⁷G. Zhang, Q. Liao, Z. Zhang, Q. Liang, Y. Zhao, X. Zheng, and Y. Zhang, *Adv. Sci.* **3**, 1500257 (2016).
- ³⁸Y. Zhao, Q. Liao, G. Zhang, Z. Zhang, Q. Liang, X. Liao, and Y. Zhang, *Nano Energy* **11**, 719 (2015).
- ³⁹Y. W. Kang, M.-J. Cho, and K.-Y. Hwang, *Water Res.* **33**, 1247 (1999).
- ⁴⁰Q. Zheng, Y. Zou, Y. Zhang, Z. Liu, B. Shi, X. Wang, Y. Jin, H. Ouyang, Z. Li, and Z. L. Wang, *Sci. Adv.* **2**, e1501478 (2016).
- ⁴¹Q. Liang, X. Yan, X. Liao, and Y. Zhang, *Nano Energy* **25**, 18 (2016).
- ⁴²Q. Zhang, Q. Liang, Q. Liao, F. Yi, X. Zheng, M. Ma, F. Gao, and Y. Zhang, *Adv. Mater.* **29**, 1606703 (2017).
- ⁴³Q. Zhang, Z. Zhang, Q. Liang, F. Gao, F. Yi, M. Ma, Q. Liao, Z. Kang, and Y. Zhang, *Nano Energy* **55**, 151 (2019).
- ⁴⁴Z. Li, H. Feng, Q. Zheng, H. Li, C. Zhao, H. Ouyang, S. Noreen, M. Yu, F. Su, R. Liu, L. Li, Z. L. Wang, and Z. Li, *Nano Energy* **54**, 390 (2018).
- ⁴⁵Q. Zhang, Q. Liang, D. K. Nandakumar, S. K. Ravi, H. Qu, L. Suresh, X. Zhang, Y. Zhang, L. Yang, A. T. S. Wee, and S. C. Tan, *Energy Environ. Sci.* **13**, 2404 (2020).
- ⁴⁶Y. Chi, K. Xia, Z. Zhu, J. Fu, H. Zhang, C. Du, and Z. Xu, *Microelectron. Eng.* **216**, 111059 (2019).
- ⁴⁷Y. Bao, R. Wang, Y. Lu, and W. Wu, *APL Mater.* **5**, 074109 (2017).
- ⁴⁸Y. Lu, X. Li, J. Ping, J. s. He, and J. Wu, *Adv. Mater. Technol.* **5**, 1900905 (2020).
- ⁴⁹K. N. Kim, J. Chun, S. A. Chae, C. W. Ahn, I. W. Kim, S.-W. Kim, Z. L. Wang, and J. M. Baik, *Nano Energy* **14**, 87 (2015).
- ⁵⁰R. Pan, W. Xuan, J. Chen, S. Dong, H. Jin, X. Wang, H. Li, and J. Luo, *Nano Energy* **45**, 193 (2018).
- ⁵¹C. Disselhorst-Klug, T. Schmitz-Rode, and G. Rau, *Clin. Biomech.* **24**, 225 (2009).
- ⁵²K. S. Türker, *Phys. Ther.* **73**, 698 (1993).
- ⁵³Q. Liang, Q. Wang, Q. Zhang, J. Wei, S. X. Lim, R. Zhu, J. Hu, W. Wei, C. Lee, C. Sow, W. Zhang, and A. T. S. Wee, *Adv. Mater.* **31**, 1807609 (2019).
- ⁵⁴Q. Liang, Q. Zhang, J. Gou, T. Song, A. Arramel, H. Chen, M. Yang, S. X. Lim, Q. Wang, R. Zhu, N. Yakovlev, S. C. Tan, W. Zhang, K. S. Novoselov, and A. T. S. Wee, *ACS Nano* **14**, 5668 (2020).
- ⁵⁵Q. Liang, J. Gou, A. Arramel, Q. Zhang, W. Zhang, and A. T. S. Wee, *Nano Res.* **13**, 3439 (2020).
- ⁵⁶Y. Yuan, R. Li, and Z. Liu, *Anal. Chem.* **86**, 3610 (2014).
- ⁵⁷X. Zhang, J. Grajal, J. L. Vazquez-Roy, U. Radhakrishna, X. Wang, W. Chern, L. Zhou, Y. Lin, P.-C. Shen, X. Ji, X. Ling, A. Zubair, Y. Zhang, H. Wang, M. Dubey, J. Kong, M. Dresselhaus, and T. Palacios, *Nature* **566**, 368 (2019).
- ⁵⁸X. Chen, Y. J. Park, M. Kang, S.-K. Kang, J. Koo, S. M. Shinde, J. Shin, S. Jeon, G. Park, Y. Yan, M. R. MacEwan, W. Z. Ray, K.-M. Lee, J. A. Rogers, and J.-H. Ahn, *Nat. Commun.* **9**, 1690 (2018).